Electronic Supplementary Material (ESI) for Polymer Chemistry.

Electronic Supplementary Information

UV-Vis/FT-NIR *in-situ* monitoring of visible-light induced polymerization of PEGDA hydrogels initiated by eosin/triethanolamine/O_2

Kaja Kaastrup[a], Alan Aguirre-Soto[a,b], Chen Wang [b], Christopher N. Bowman [b], Jeffery Stansbury[b,c], Hadley D. Sikes [*a,d]

[a.] *Department of Chemical Engineering, Massachusetts Institute of Technology, Cambridge, MA 02139, United States*
[b.] *Department of Chemical and Biological Engineering, University of Colorado Boulder, 3415 Colorado Ave., Boulder, Colorado 80303, United States*
[c.] *Department of Craniofacial Biology, School of Dental Medicine, University of Colorado, 12800 East 19th Ave., Aurora, Colorado 80045, United States*
[d.] *Program in Polymers and Soft Materials, Massachusetts Institute of Technology, Cambridge, MA, 02139, United States*

* Correspondence: sikes@mit.edu

Table S1. Baseline shift and curing light contamination: transition times

Intensity (mW/cm^2)	**Time (A_{500}/ A_{523} maximum of 2nd derivative) (seconds)**		**Time (μ'_S maximum) (seconds)**	
	Ambient	Argon-purged	Ambient	Argon-purged
1.5	389 ± 22.5	195 ± 33.0	373 ± 37.9	181 ± 29.5
3.7	235 ± 15.1	178 ± 18.6	230 ± 11.8	147 ± 12.6
6	191 ± 23.6	120 ± 6.8	173 ± 29.5	111 ± 6.4
9.6	184 ± 52.1	98 ± 16.9	153 ± 29.5	103 ± 9.8

Table S2. Baseline shift and curing light contamination: conversion at transition times

Intensity (mW/cm^2)	**Vinyl Fractional Conversion (A_{500}/ A_{523} maximum of 2nd derivative)**		**Vinyl Fractional Conversion (μ'_S maximum)**	
	Ambient	Argon-purged	Ambient	Argon-purged
1.5	0.31 ± 0.04	0.35 ± 0.02	0.27 ± 0.03	0.33 ± 0.02
3.7	0.38 ± 0.01	0.34 ± 0.01	0.37 ± 0.003	0.31 ± 0.01
6	0.35 ± 0.01	0.31 ± 0.01	0.33 ± 0.01	0.30 ± 0.01
9.6	0.33 ± 0.04	0.29 ± 0.03	0.30 ± 0.02	0.29 ± 0.02

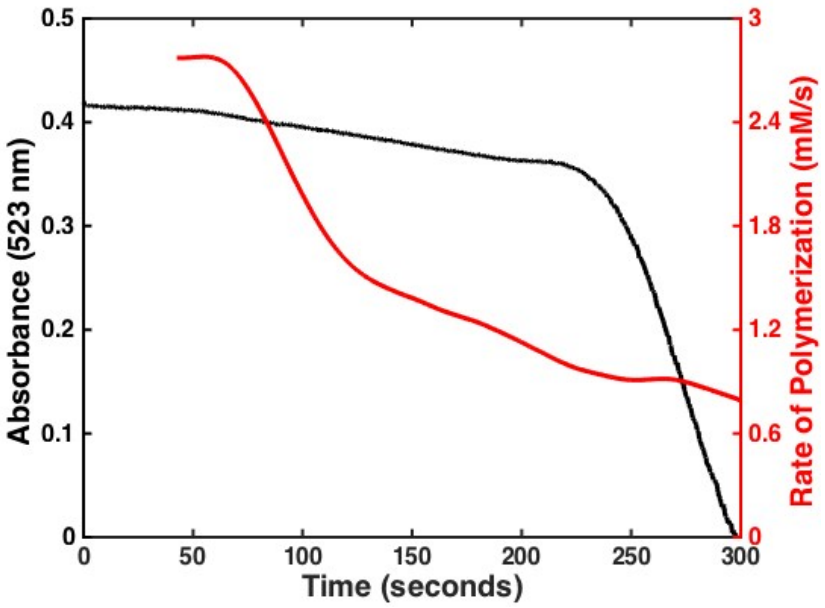

Fig. S1. Baseline corrected absorbance for the eosin ground state at 523 nm (black) and the rate of polymerization (red) as a function of time.

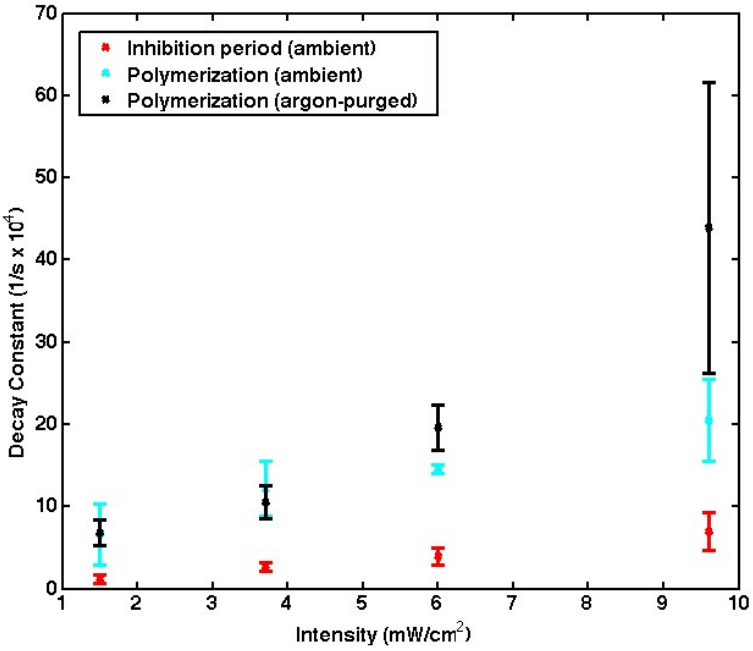

Fig. S2. Exponential decay constants (τ, $A(t) = A_0 e^{-\tau t}$) for ambient and argon-purged conditions as a function of curing light intensity.

Table S3. Exponential decay constants for ambient and argon-purged conditions at different curing light intensities (tabulated data from Fig. S2)

Intensity (mW/cm²)	**Inhibition Time (seconds)**		**τ (inhibition period, 1/s x10⁴)**	**τ (polymerization, 1/s x10⁴)**	
	Ambient	Argon-purged	Ambient	Ambient	Argon-purged
1.5	142 ± 25	17.8 ± 2.7	1.2 ± 0.5	6.6 ± 3.7	6.8 ± 1.5
3.7	42.2 ± 1.2	5.6 ± 2.4	2.7 ± 0.5	12.2 ± 3.3	10.5 ± 2.0
6	27.7 ± 4.0	0	4.0 ± 1.0	14.6 ± 0.5	19.6 ± 2.8
9.6	20.0 ± 3.5	0	7.0 ± 2.3	20.5 ± 5.0	43.9 ± 17.7

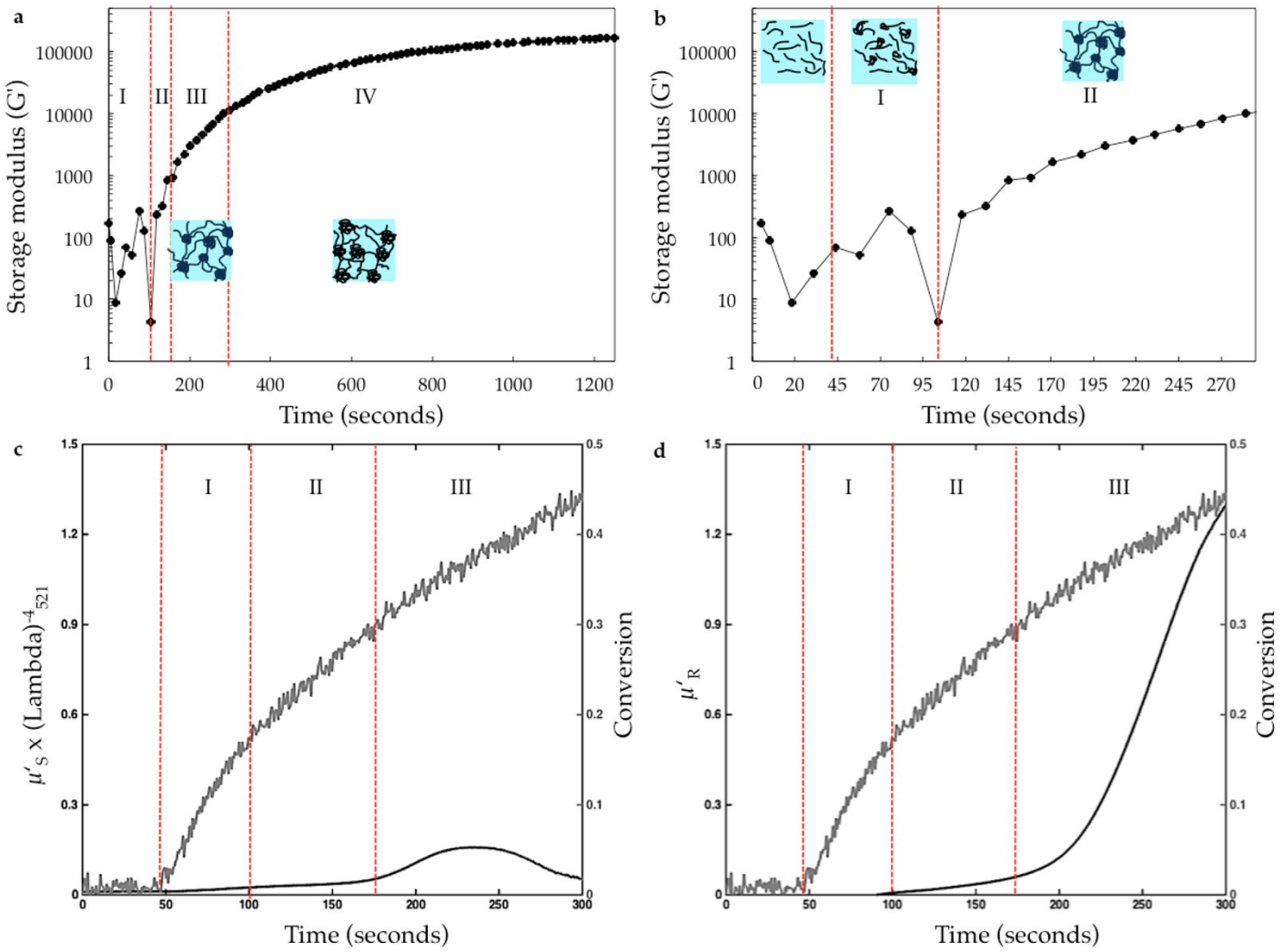

Fig. S3. a & b) Storage modulus G´ (Pa) vs irradiation time for the photopolymerization of a solution containing eosin, TEA, VP, and PEGDA in water in the presence of oxygen with 500 nm irradiation (3.7 mW/cm^2, LED source). c & d) Correlation with the evolution of μ'_S and μ'_R (extracted from Figure 3)..Pictorial representations of the hydrogel structure during the different regions were extracted from Figure 2.

After the inhibition period, four regions can be identified from the μ'_S and μ'_R plots (divided by the red dashed lines): I) where μ'_S accounts for all the optical attenuation, II) where both μ'_S and μ'_R increase slowly at equivalent rates, III) where μ'_S goes through a maximum before going back to μ'_S=0 and μ'_R increases drastically, and IV) where μ'_S remains equal to zero and μ'_R slowly reaches a plateau. We can then correlate these four regions to the storage modulus. During region I, the storage modulus remains within the initial noise value of 100 Pa until ~ 100 s of irradiation while μ'_S increases slightly and μ'_R=0. Region II coincides with the onset of μ'_R , which suggests that μ'_R has a stronger effect on the modulus than μ'_S. During region II μ'_S and μ'_R slowly become equivalent in terms of their contribution to the optical attenuation, while G´ increases sharply. In region III, both μ'_S and μ'_R initially increase while the rate of increase in G´ slows down. At 235 s μ'_S reaches a maximum and begins to decrease back to zero, while the contribution of μ'_R to the optical attenuation increase even more and becomes close to 100% of the total attenuation value. Meanwhile, the rate of G´ as a function of time decreases further. Finally, in region IV both G´ and μ'_R slow down until reaching plateau values. These observations suggest that μ'_R is closely linked to the formation of a macrogel that contributes to the overall mechanically robustness of the hydrogel. In contrast, μ'_S has a weaker correlation to G´, which appears to indicate that the λ-dependent component of the optical attenuation is due to the initial formation of nanogels and their clustering up to the point where swelling dominates and leads to macrogelation, which results in the development of a mechanically robust hydrogel with a final G´ value over 1 MPa.